[Frontiers in Bioscience 2, a1-10, January 1, 1998]

OPTICAL SPECTROSCOPY OF BREAST BIOPSIES AND HUMAN BREAST CANCER XENOGRAFTS IN NUDE MICE

Fay A. Marks, Ph. D.

General Electric Corporate Research and Development, One Research Circle, Niskayuna, NY 12309

Received 11/25/97 Accepted 12/5/97

TABLE OF CONTENTS

1. ABSTRACT

The optical response of benign and malignant breast biopsies was recorded using a double beam, ratio-recording UV_VIS_NIR spectrophotometer equipped with a 150 mm diameter integrating sphere. Differences in the oxygenation state of hemoglobin for benign and malignant breast biopsies were found. Specifically, spectral component analysis performed in the 300 - 800 nm wavelength region showed that the malignant samples contained predominantly deoxygenated blood while the benign samples exhibited oxyhemoglobin resonances exclusively. Fibroadenoma, a benign tumor, was found to exhibit a deoxyhemoglobin signature and was thus indistinguishable from cancer. Fibroadenoma is also a false positive for X-ray mammography and contrast-enhanced MRI. The *in vitro* experiments were repeated *in vivo* using a remote reflectance spectrophotometer and human breast cancer xenografts implanted in nude (immune-deficient) mice. The *in vivo* studies confirm that (1) a potentially exploitable difference in the functional utilization of oxyhemoglobin exists between benign and malignant breast processes, and (2) the sample collection and *in vitro* preparation protocols yield tissue samples that adequately represent (spatial) average functional behavior *in vivo*. It is postulated that these differences may serve as the basis for the non invasive, differential diagnosis of benign and malignant breast processes, or, for tissue characterization in a minimally invasive environment.

2. INTRODUCTION

Conventional X-ray mammography is the 'gold standard' for breast cancer imaging. It is currently unmatched in its ability to detect and diagnose cancer in symptomatic and asymptomatic women. However, X-ray mammography has a number of limitations which reduce its effectiveness under certain conditions. A case in point is the radiographically dense breast which poses a significant problem to the radiologist. The reason for this is that tumors are typically as radiodense as normal fibroglandular tissue and there is very little fat present in the dense breast to provide contrast on the X-ray mammogram. This makes it very difficult to return a diagnosis with a high degree of confidence. Current clinical solutions to this particular problem include additional X-ray views, supplemental ultrasound, and correlation with breast physical exam. New technologies like optical biomedical imaging are being investigated as possible solutions to this and other breast imaging issues.

The major approaches to optical biomedical imaging include Phase Modulation Spectroscopy (1-2), Time Resolved Spectroscopy (3-6), Optical CT (7) and Ultrasound Assisted Optical Imaging (8-11) with applications ranging from hypoxic brain injury to neonatal monitoring to breast cancer imaging. Some researchers are pursuing the differences found between the native fluorescence (12-15) and absorption of normal tissue and carcinoma as the basis for cancer discrimination, while others are investigating the utility of exogenous contrast agents. All optical avenues to breast cancer imaging have their pros and cons. This researcher has chosen the road without contrast agents because the subpopulation of symptomatic women who cannot tolerate contrast agents is growing, making it imperative that alternatives to contrast agent-based breast imaging be vigorously pursued.

GE is using ultrasound-assisted optical imaging as the basis for a spectroscopy-at-a-voxel imager in an attempt to combine imaging with spectroscopy for greater detection efficacy, and, to address the problem of the radiodense breast. It is expected that contrast in this system will, in the main, be provided by spectral discrimination. The work reported here deals only with the spectroscopic component of the system, and investigates the potential of optical spectroscopy as a functional imaging tool, by looking at the *in vitro* and *in vivo* optical responses of breast biopsies and human breast cancer xenografts in the visible and near infrared wavelength regions. This paper will show that light can provide tissue characterization in the radiographically dense breast. The benefits of such a diagnostic tool using non-ionizing radiation are self evident.

3. MATERIALS AND METHODS

For studies of this kind, where an indirect marker of pathology is sought, the ultimate goal would be to use models which mimic the *in vivo* physiological conditions under investigation. The experimental nature of the hunt in this case precluded human studies, so the samples used in this study are tissue specimens which represent, as nearly as possible, the metabolic function of the tissue under normal physiological conditions. The studies described here move though two phases. The existence of exploitable, functional effects is investigated by first examining the *in vitro* spectral response of breast biopsies and human breast cancer xenografts (16-17), collected and harvested according to a strict protocol. Then, in a follow-on phase, measurements of human breast cancer tumors are performed *in vivo* in nude mice to test the *in vitro* experimental findings.

3.1. *In Vitro* Experimental Method

Thirty-four breast biopsies (11 malignant, 4 fibroadenoma, 3 male breast gynecomastia and 16 fibrocystic & other benign breast processes), twenty-five mouse model tumors stored in growth medium, and 1 gm of cancer cell cultures were studied. The sizes of the biopsies ranged roughly from a few millimeters to 1 cm and the sizes of the mouse model tumors ranged from about 4 mm spheroids to sections roughly 3 cm in diameter.

Sample collection and handling was designed to acquire samples that would mimic metabolic function under *in vivo* conditions as closely as possible within the scope of the study. The samples chosen to best represent these conditions were: (1) breast biopsies frozen (at -70 °C) within 5 - 10 minutes after removal from the host, (2) mouse model tumors, harvested immediately after sacrifice and stored in growth medium at wet ice temperatures, and (3) approximately 1 gm of a viable culture of cancer cells. The breast biopsies were obtained from a local hospital: Ellis Hospital in Schenectady, NY. The human breast cancer xenografts were grown in nude mice at the UCLA Medical Center in California, harvested and shipped to Schenectady in wet ice, and the cancer cell cultures were prepared at Rensselaer Polytechnic Institute in Troy, New York.

Prior to spectrophotometry, the breast biopsies were maintained in the laboratory at or below -50°C and the mouse model tumors were kept in growth medium either at 0 °C or at -50°C. The cancer cells were washed in phosphate buffer and spun down into a pellet. The pellet was placed in a quartz cuvette with a 1 mm path length. The biopsy samples and mouse model tumors were cut in a Nitrogen atmosphere while still frozen, to the desired thicknesses ranging from approximately 25 microns to 5 mm, and placed between quartz microscope slides with appropriate spacers. Care was taken to drain all samples after mounting and prior to measurement to get rid of any excess fluid and growth medium, which has absorption resonances in the visible that overlap those of tissue. As a control check, a few model tumors were snap frozen with liquid nitrogen (LN_2) after removal from the host, and their spectra compared with those of tumors stored in growth media. For selected samples, pathology was performed on material adjacent to and within 2 mm of the piece under study to eliminate errors of identification due to heterogeneity in large samples. As a final step in minimizing the time between sample collection and measurement, the optical spectra of the tissue samples were recorded typically within two to ten minutes after removal from dry ice storage or growth medium.

A Hitachi 3410 UV-VIS-NIR spectrophotometer with integrating sphere was used to measure the optical response of the tissue samples. The spectrophotometer is a double beam, ratio-recording instrument equipped with a system of detectors and lamps which permits the uninterrupted monitoring of wavelengths from 240 nm to 2500 nm. The use of the integrating sphere allowed us to collect all of the light scattered through 180 degrees in the back plane of the turbid sample.

Transmittance measurements were taken, and two types of scans were recorded for each tissue sample: a spectrum from 240 nm to 2500 nm and a narrow scan from 240 nm to 700 nm. For the narrow scans, improved resolution and signal-to-noise was achieved using a 1 nm bandpass and signal averaging of at least five repeated scans. Quantitative analysis of the spectra was performed on the average of the narrow scans using the Hitachi software package, Spectracalc.

3.2. *In Vivo* Experimental Method

Nineteen nude mice were implanted with four human breast cancer cell lines: Mitchell, UCLA #157, UCLA #645 and UCLA #231. The cells were implanted subcutaneously on the back and intramuscularly on the hind leg. The heterotransplantations were performed at UCLA in the laboratories of D. J. Castro, M.D, Ph. D and R. Saxton, Ph. D. The implantation schedule was staggered in an attempt to produce tumors at various stages (18) of growth: UCLA cell lines #231 and #645

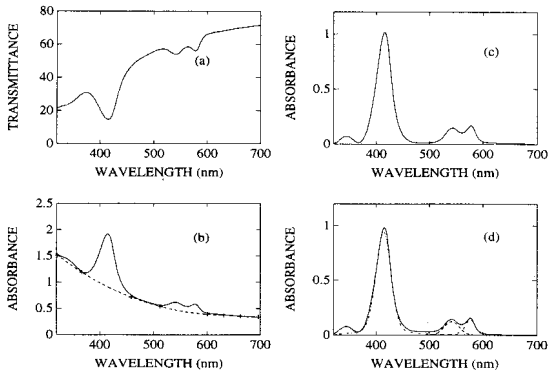

Figure 1. *Data manipulation.* (a) Transmittance spectrum as collected. (b) Converted to absorbance [A = - ln(T)]. (c) Light scattering background (----) subtracted to yield 'pure' optical absorbance spectrum. (d) Deconvolution of absorbance spectrum yields four absorption resonances.

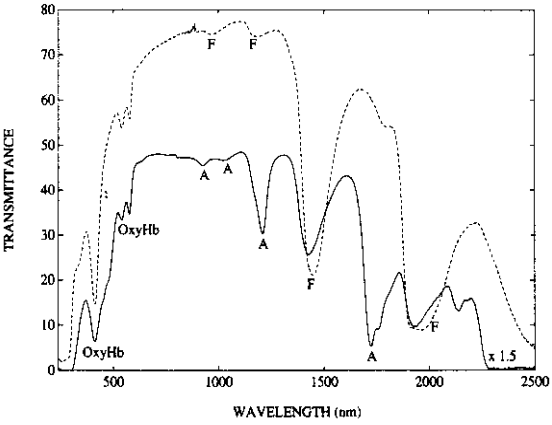

Figure 2. Optical Transmittance through 3 mm of adipose breast biopsy and 500 microns of fibroglandular breast biopsy (----). The absorption peaks marked F and A are due to fibroglandular and adipose tissue respectively. The absorption resonances marked 'OxyHb' are hemoglobin resonances in the tissue.

were implanted in two mice each every Monday for four weeks. These tumors were studied twice within a 2-week time period beginning the week of the last implantation. The other two cell lines were implanted and allowed to grow for approximately four weeks.

A remote VIS-NIR model 260 Guided Wave Spectrophotometer was used in conjunction with a 7:7 bundle fiber reflectance probe to perform the *in vivo* optical studies of the model tumors. Reflectance spectra were recorded over the wavelength range 350 - 1000 nm in 1 nm steps. The reflectance probe delivered ~ 9 mW of white light to the tumors through seven fibers and collected the reflected light from the tumors with seven fibers. This reflected light was then passed through a monochromator with a 0.5mm slit to a silicon detector and recorded. The diameter of the fiber bundle was approximately 2 mm.

Optical reflectance measurements were taken by touching the probe against the tumors with firm, but moderate pressure. Depending on the size of the tumor relative to the probe, measurements were taken at at least two different positions on the tumors. For each measurement, three to five consecutive scans were recorded as a reproducibility check and for off-line averaging. Measurements were taken in two cases: (i) with the skin over the tumor intact, and (ii) with the tumor exposed by raising a flap of skin over the lesion. In the first case, the mouse was awake and allowed to sit quietly during data acquisition; in the second case, the mouse was anesthetized throughout the entire procedure. After data acquisition, the flap of skin was repositioned and sutured and the mouse allowed to recuperate, making it possible for further measurements on that particular tumor at a later date.

4. RESULTS AND DISCUSSION

4.1. *In Vitro* Studies

As stated in Section 3.1, pathology was performed on tissue sections within 2 mm of the tissue volume probed by optical spectroscopy in order to double check the pathology of the sample under study. Any miscoded samples, or samples that either did not conform to preparation and handling protocols or were demonstrated via pathology to be subjected to substandard handling were discarded. Further, only those malignant samples demonstrated by pathology to have little or no other tissue types present were included.

The transmittance spectrum through a typical tissue specimen is composed of absorption resonances superimposed on a smoothly varying background caused by light scattering. For the narrow scans, each spectrum was manipulated as shown in figure 1. Transmittance (T) data were converted to absorbance A, where A = - ln (T), and the scattering background was removed by first fitting and then subtracting a fifth order polynomial from the absorbance data. Finally, using a combination of Gaussians and Lorentizians, the best least squares fit of the sum of these peaks to the background corrected experimental data was obtained. The approach taken was to use the least number of peaks that would adequately fit the data and still yield a reasonable physical solution, i.e a peak was deemed real if its existence was obvious by inspection or, if it corresponded to the absorption of a biological chromophore known to be present in the sample.

4.1.1 Breast Biopsies

The dominant features in the spectra of the biopsies are water absorption peaks, absorption peaks attributable to fat, and hemoglobin absorption peaks. It was quickly established (figure 2) that adipose and fibroglandular tissue are very easily distinguished by optical absorption spectroscopy. The 3 mm thick adipose tissue sample in figure 2 absorbs at 920, 1036, 1203 and

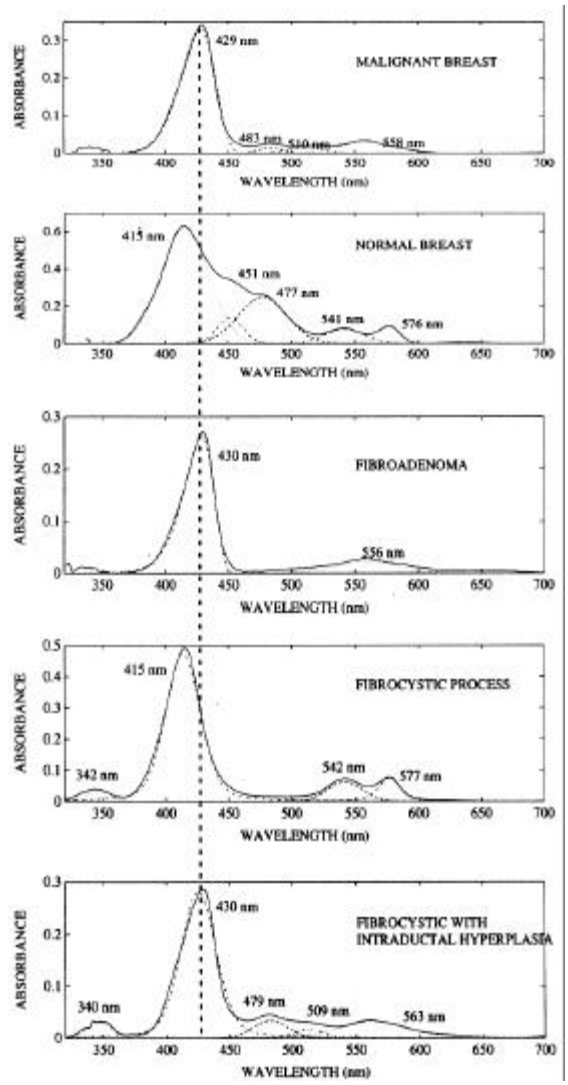

Figure 3. Absorbance spectra of malignant and benign breast biopsies. Malignancies exhibit a deoxyhemoglobin spectral signature, while normal tissue and fibrocystic disease, a benign breast tumor sometimes coded as malignant on x-ray mammograms, both exhibit an oxyhemoglobin spectral signature. Fibroadenoma, a mammography and MRI false positive, exhibits a deoxyhemoglobin spectral signature similar to the malignant breast. In fibrocystic disease with intraductal hyperplasia, the spectral response is mixed, but the deoxyhemoglobin optical signature dominates the spectrum.

1724 nm, while the 500 micron thick fibroglandular sample exhibits water peaks at 965, 1177, 1441 and 1945 nm. The shape of the background in each spectrum carries a clue about light scattering in the sample especially below 1000 nm. It is interesting to note that for adipose tissue, even a sample six times as thick as a fibroglandular specimen does not scatter light as strongly as fibroglandular tissue. So, not only are light absorption resonances characteristic of tissue type but so is light scattering within the sample.

There is a transmission window from 600 nm to 1000 nm where the highest percentage of light is transmitted through biological tissue. Contributors in the field have typically looked only in this region for spectral features which can discriminate normal from malignant tissue. Unfortunately, within the sensitivity limits of the spectrophotometer, there are no easily observable chromophores (distinct from hemoglobin) that absorb in this wavelength region that can be used as a cancer marker. The region above 950 nm is dominated by broad water absorption peaks, and the region below 600 nm is dominated by the hemoglobin absorption resonances. If there are any spectral features above 1000 nm that are different for different breast tissue types, they will be masked by the water absorption peaks. However, there are differences that are observed below 600 nm that separate cancer from normal tissue. These are differences in the oxygenation saturation state of hemoglobin within the tissue.

The absorption spectra in figure 3 compare the spectral responses of breast cancer with 'normal' breast tissue and certain benign conditions. Essentially, breast cancer exhibits a deoxygenated hemoglobin (Hb) signature while normal tissue exhibits an oxygenated hemoglobin (HbO_2) signature. The Soret band of 100% oxygen saturated hemoglobin appears at 415 nm and the characteristic alpha and beta bands appear at 577 nm and 542 nm respectively (19). The spectrum of pure deoxygenated hemoglobin is completely different; the Soret band is red shifted to 431 nm and the region of the alpha and beta bands is replaced by a single broad resonance at 555 nm. There is also a much weaker, but characteristic absorption peak at 760 nm.

Component fitting was used to determine peak positions and peak widths of the tissue absorption resonances by assuming a combination of Gaussians and Lorentzians for the peak shape. The hemoglobin Soret band is clearly asymmetric, but no attempt was made to include an asymmetry factor or to derive any information from variations, if any, in such a parameter. An unidentified peak at 512 nm was observed in the biopsy cancer samples that did not appear in the normal or benign tumor specimens. Though this resonance at first glance appears to be an additional means of cancer discrimination by optical spectroscopy, it is extremely weak and probably has limited utility pending its identification. The results of component fitting also reveal in some of the samples, traces of bilirubin, which absorbs in the blue at about 452 nm, and a transition at about 480 nm tentatively assigned to fat absorption.

Figure 3 shows that the spectral signature of fibroadenoma, a mammography false positive, is very similar to that for cancer except for the 512 nm peak. On the other hand, optical spectroscopy can clearly distinguish fibrocystic disease, another mammographic false positive, and in fact does indicate through variations in spectral shape and peak position, the presence of intraductal hyperplasia. These *in vitro* findings strongly suggest that optical spectroscopy, which measures spatially averaged

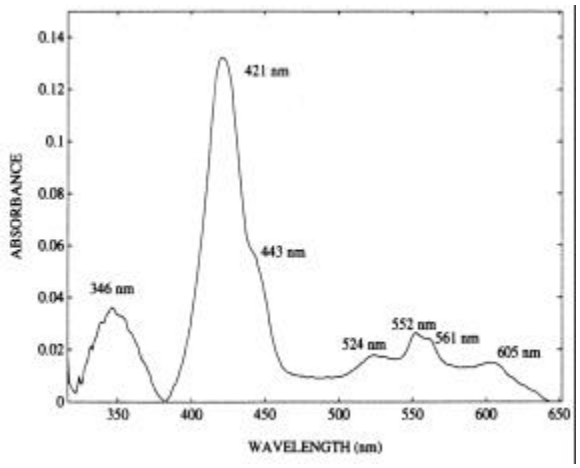

Figure 4. Absorption spectra of approximately 0.5 gm of viable cancer cells.

tissue function, may be useful in non invasive tissue diagnostics.

The fact that malignant tumors differ from normal tissue and benign tumors in the oxygenation state of hemoglobin, could be due in part to the differences in blood flow rates and therefore oxygen consumption rates (20) of the various tissue types. Studies on the nature of tumor hypoxia have been going on for decades (21), usually in connection with efficacy of radiation treatment.

4.1.2. Human Breast Cancer Xenografts

Three human breast cancer cell lines were implanted into nude mice at UCLA Medical Center in California: #231, #645 and Mitchell. These model tumors were harvested and shipped in growth medium to my lab at wet ice temperatures. On inspection, it was determined that the spectra of LN_2 snap frozen tumors and tumors stored in growth media were very similar, proving that the preparation and treatment of the latter was adequate. Irrespective of size, all of the twenty-five tumors studied with one exception, exhibited deoxygenated hemoglobin signatures. The last cell line, the UCLA Mitchell, was very difficult to grow in the host mouse so, only two tumors in this cell line were studied; one had a HbO_2 signature. In none of the model tumors studied was the 512 nm resonance evident. In the model tumors, the cells are human breast cancer cells, but the surrounding stroma and blood vessels are provided by the mouse. Thus it is possible that the 512 nm peak is indicative of the host response which may not be accurately modeled in the mouse.

The optical response of the model tumors grown from human breast cancer cell line #231 was different from that of the other model tumors. The peak positions of the hemoglobin resonances of the #231 tumors appeared at 430 nm and 555 nm on the average, much like those of the malignant breast biopsies. One of the Mitchell tumors and all of the #645 model tumors on the other hand, exhibited resonances in the Soret region ranging from 420 nm to 425 nm, and a broad resonance in the alpha and beta region with features at 523 nm, 552 nm, 561 nm and 604 nm. When compared with the spectra from the live cancer cell cultures, it is apparent that these features can be attributed to the respiration enzyme cytochrome oxidase. Visual inspection of the tumors revealed that while the #231 tumors looked like breast biopsies with surrounding stroma and blood vessels, the Mitchell and #645 tumors looked like spheroids of cells with little or no blood vessels. Clearly then, this accounts for the spectral differences in the cell lines since with little or no blood present, cytochrome oxidase will dominate the Mitchell and #645 spectra, and for the blood perfused #231 tumors, hemoglobin will dominate the spectra. It appears that UCLA was able to grow and maintain spheroids of human breast cancer cells in nude mice with minimal support from the host. Further, since these tumors were studied as soon as received with no treatment other than having been stored in growth medium at wet ice temperatures for about 24 hours, it is believed that they were viable at the time of study, even if somewhat hypoxic.

4.1.3. Breast Cancer Cell Cultures

Approximately one gram of cancer cells (UCLA cell line #231) was incubated, pelletized and placed in a quartz cuvette. Figure 4 shows the absorption spectrum of these cells. Since there is no hemoglobin in the cells and since the phosphate buffer used for washing the cells does not have an optical signature in the visible region, the absorption resonances are from the cancer cells alone. The peaks displayed are from the terminal respiration enzyme cytochrome oxidase. Though the Soret peak of cytochrome oxidase is normally masked in the model tumors and biopsy samples by strong hemoglobin absorption, it may be sufficiently strong to change the symmetry of the hemoglobin Soret of the breast tissue samples. No attempt was made to fit the asymmetry of the Soret band of the breast biopsies by trying to compensate for the presence of cytochrome oxidase absorption resonance.

4.2 *In vivo* Studies

The tumors that were implanted intramuscularly on the hind leg were difficult to assess. In some cases, the tumors were buried within the muscle; in other cases, part of the white lesion could be visually located at the surface of the muscle. Although optical measurements were taken of both the intramuscular and subcutaneous tumors, no attempt was made to draw conclusions from the former case.

The tumors implanted subcutaneously on the back were fed by blood vessels in the skin. They tended to be encapsulated within a translucent film and were surrounded by a sheath of blood vessels; a single main vessel feeding the tumor was usually clearly evident especially in the larger (>0.5 cm) tumors. These cancers did not invade the back tissue, however, depending on the physical distribution of the cells at transplantation, some tumors extended down the length of the back and some

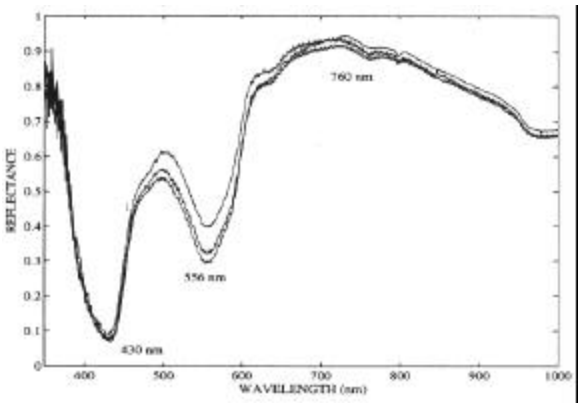

Figure 5. *In vivo* optical reflectance spectra of a human breast cancer xenograft (UCLA #645 cell line) 8 days after subcutaneous heterotransplantation into a nude mouse. Tumor size:7mm x 4mm x 4mm.

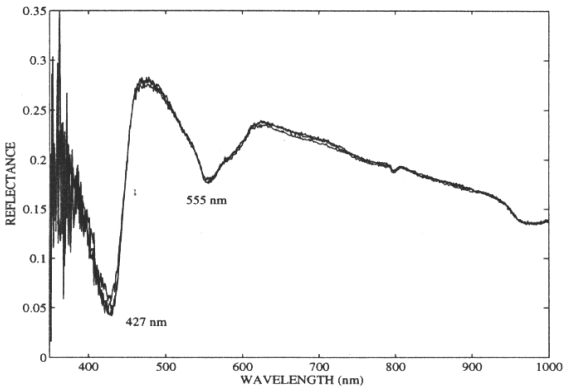

Figure 6. *In vivo* optical reflectance spectra of a human breast cancer xenograft (UCLA #645 cell line) 29 days after heterotransplantation into a nude mouse. Tumor size: 20mm x 17mm x 10mm.

remained localized at the implantation site. The skin over the model tumors implanted on the back varied in thickness from <250 microns to 1mm depending in part on the size of tumors. The skin over the tumor was necrotic in some areas for some of the lesions. Whenever this occurred, an incision was made in the skin at the base of the tumor and (since in most cases, the skin adhered to the tumor), both skin and tumor were raised to allow measurements to be taken on the underside of the tumor. The procedure was performed in such a way as to minimize bleeding. Care was taken to prevent any blood from the incision in the skin from contaminating the area of the tumor selected for measurement, and, prior to measurement, the sheath of blood vessels surrounding the tumor was carefully pushed aside.

We will confine ourselves to a discussion of the optical response of exposed subcutaneous tumors. The decision to remove a flap of skin to uncover the tumors was made with two objectives in mind: (i) to exclude the contribution from the skin for ease of data interpretation and (ii) to remove the risk of being limited by the penetration depth of light within tissue. The geometry of the 7:7 fiber optic probe used restricts the penetration depth of the light to about 8mm. However, since we are monitoring the reflected light, our actual probe volume is much smaller. This probe depth was estimated using the following simple experiment. *In vitro* samples of model tumors (previously harvested and stored in dry ice) were placed between two quartz slides with spacers. A wavelength reflectance filter was placed behind the model tumor specimens, and the 7:7 reflectance bundle probe illuminated the slab of tumor from the front. The probe, the slab of model tumor and the filter were placed in direct contact with each other and the response of the signal from the filter (at its specific stop-band wavelength) to increasing sample thicknesses was monitored. The thickness at which the signal from the filter almost disappeared was recorded as the depth in tissue from which useful information was received at that specific wavelength for the reflectance probe geometry used. The probing depths were recorded for three wavelengths: 420 nm (Soret region), 540 nm (in the region of the alpha and beta hemoglobin bands) and 750nm which is close to the deoxyhemoglobin resonance at 760 nm. The approximate depths were 0.5, 1.5 and 2mm respectively.

Typical reflectance spectra from an exposed back tumor are shown in figure 5. The reflectance units are not absolute. Several diffuse standards were tested in the field, but since none were effective as a reflectance standard with the geometrical configuration used, a mirror was used as reference. For this reason, the reflectance of the tissue as recorded, not surprisingly, is less than one percent. This less than optimum choice of reflectance standard does not affect our results, since we are not attempting quantitation, but rather simply the qualitative identification of the oxidation state of hemoglobin in the tissue.

Three consecutive scans were recorded in figure 5, each scan lasting approximately one minute. This particular example of *in vivo* experimental data was taken on the eighth day after subcutaneous implantation of UCLA #645 cancer cells, when the tumor was 7mm x 4mm x 4mm in size. The tumor's optical reflectance spectrum qualitatively resembles that of completely unsaturated hemoglobin. These spectra also demonstrate the high degree of reproducibility of the optical measurements from the nude mice and confirms that the data collection protocols (e.g. mouse handling and probe pressure by operator) were adequately implemented. Another tumor grown from the same cell line is shown twenty-nine days after subcutaneous in figure 6. This large (20mm x 17mm x 10mm) tumor also exhibits a deoxyhemoglobin spectral signature. Both of the tumors in figure 5 and 6 were in direct contact with the fiber optic probe. In both cases, minimal bleeding occurred at the incision, and the probe area itself was not contaminated.

Five mice without tumor implants were used as controls. A small flap of skin was raised over the back of the anesthetized mouse and the reflectance spectra recorded. The

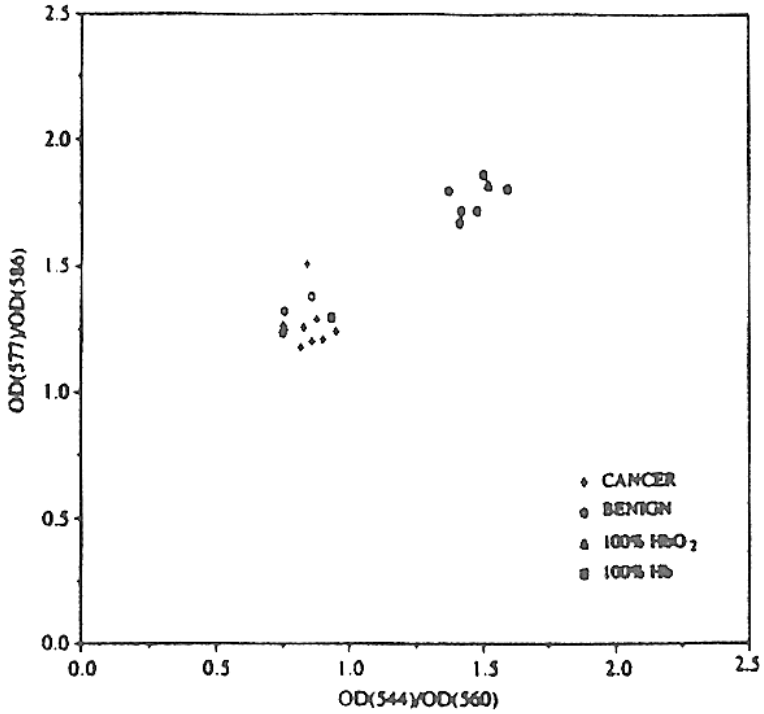

Figure 7. Scatter diagram showing the separation of malignant from benign breast processes using biopsy breast tissue. (See text.)

skin flap was sutured back into place after the measurement and the mouse allowed to recuperate. Without exception, the sites monitored exhibited an oxyhemoglobin spectrum. So, we conclude that the measurement and mouse handling protocols did not cause desaturation of hemoglobin, which effect would mimic the signals from the tumors.

The influence of applied pressure to the tumor on the reflectance spectrum from the mice was addressed by sensitizing the operator holding the mice against the probe to how much pressure could be applied without corrupting the reflectance data. A series of tests involving varying the pressure of the probe on the operator's hands and fingers and on the mice themselves indicated that it was indeed possible to distort the reflectance spectrum if too much pressure was applied to the area of interest. Conversely it demonstrated that there is a 'safe' pressure range, and that once the operator maintained that pressure for the mice studied, it was possible to collect uncorrupted data. Further, the system was demonstrated to be very sensitive to positional changes of the mouse, and to operator motion. If any of these disruptions occurred during data acquisition, it was reflected in the data and the data was discarded. It should be noted here that not even under conditions of extreme application of pressure could we generate deoxyhemoglobin signatures.

Figure 5 exemplifies a more benign form of body motion that was tolerated. The ripple present on the spectrum in the near infrared is not due to system noise, but rather to the involuntary shivering of the mouse. That the absorption features are not affected by this kind of motion was verified in a few of the mice in which shivering during data acquisition occurred. The mouse in figure 6 was not shivering during data acquisition.

The most important result of this *in vivo* study is that statistically, the model tumors presented significant regions of completely unsaturated hemoglobin, confirming the *in vitro* experimental results. Figures 5 and 6 show that this tendency to oxygen depleted hemoglobin may be found not only in large, advanced tumors but also in small, early (8 days old) tumors. The smallest tumor evaluated was a flat, round 4 mm lesion (15 days old), and this too had a deoxyhemoglobin optical signature. Another finding of import was that the tumors were in fact heterogeneous with respect to hemoglobin oxygen saturation; of the several positions on the exposed surface of the larger tumors that were monitored, most exhibited a desaturation of the hemoglobin. At some positions however, the tumor had an oxyhemoglobin signature. What this tells us is that while optical spectroscopy as implemented here presents a possible marker for lesion location, demarkation of tumor borders would not be possible.

4.3. Spectral Discrimination

An obvious way to quantify these experimental findings would be to measure the actual oxygen saturation of hemoglobin in the excised tissue and in the model

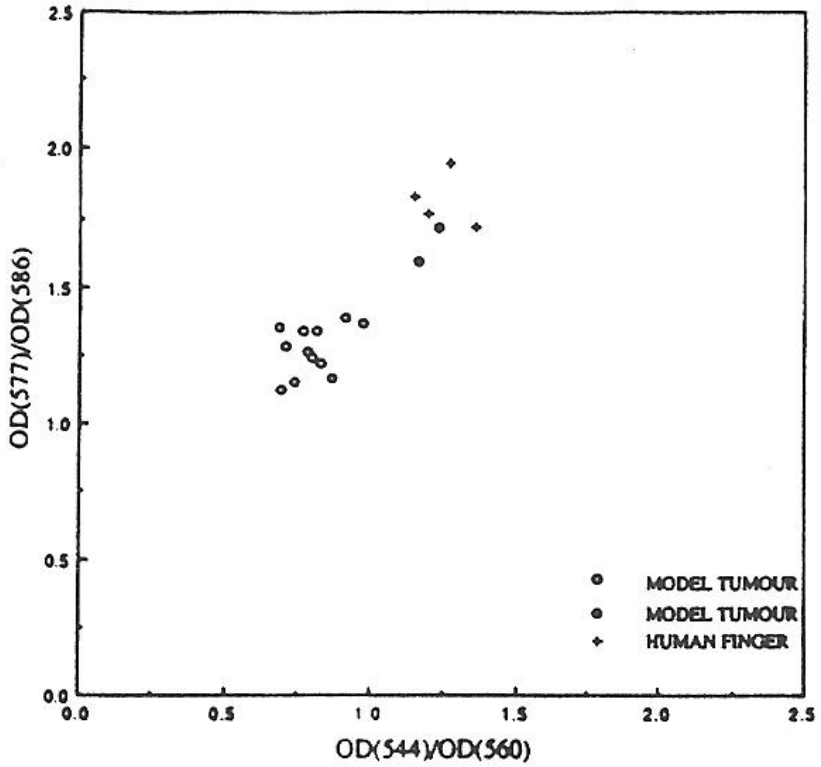

Figure 8. Scatter diagram showing the clustering of human breast tumor xenografts *in vivo* and the separation of the tumor cluster from that of the controls. (See text.)

tumors *in vivo*. In order to do this, we would need to compensate for the presence of cytochrome oxidase and other chromophores like bilirubin in the spectra. Since this was outside the scope of the studies, we elected to display the spectral differences between cancer and benign breast processes on a scatter diagram using ratios based on the oxygenation state of the hemoglobin. The scatter diagram for the *in vitro* samples is shown in figure 7 which plots the ratio of absorbances at 544 nm and 560 nm (an isosbestic point) against the ratio of absorbances at 577 nm and 586 nm (an isosbestic point). For clarity, only a few of the samples studied are represented on the diagram. The isosbestic points were used to normalize the data and correct for the difference in blood volumes that existed from sample to sample. In the figure, the circles represent the benign samples (which include normal and benign tumors) and, the plusses represent the malignant samples.

As a benchmark, the triangle and the square represent values which correspond to human tissue with physiological levels of hemoglobin oxygen saturation and completely desaturated blood, respectively. These values were obtained by creating laboratory models of these two types of functional conditions. First, a blood donor inhaled pure oxygen for five minutes. Then blood was drawn to capture a blood sample at physiological levels of oxygen saturation. This sample was split into two, and one part (7ml.) was deoxygenated by adding an excess of sodium dithionite (30 mg). Then, ideal tissue phantoms of normal tissue and malignant tissue (suitable for absorption spectroscopy) were created by adding a drop of the oxygenated whole blood sample to a cuvette of viable pelletized cancer cells, and a drop of the deoxygenated whole blood sample to a second cuvette of viable pelletized cancer cells. Two oxygenated tissue phantoms and three desaturated tissue phantoms were created in this fashion. The appropriate averages of optical spectra collected from these phantoms were taken, and the absorbance ratios calculated from these averages.

A quick examination of figure 7 reveals that the benign and malignant samples separate into clusters in the vicinity of the appropriate calibration data points corresponding to the tissue phantoms. It can also be seen that three of the benign samples fall in the malignant cluster; these correspond to two fibroadenoma samples and the single case of fibrocystic disease with intraductal hyperplasia studied.

Figure 8 shows a similar cluster diagram for the *in vivo* results. In this case also, we find that the tumors cluster and are separate from the cluster of 'normals'. The 'normal' control samples in this case were the hands and fingers of volunteers; it is not

possible to grow benign tumors in the nu/nu hemozygotes. The assumption made here is that the spectra of normal hands and fingers are similar to normal breast tissue. When compared with the *in vitro* results in Figure 7, it is immediately obvious that the *in vivo* model tumors and the volunteers are less tightly clustered and the separation between them less distinct than in the *in vitro* case. This is not surprising as one would expect to record far more spread in the hemoglobin oxygenation *in vivo* than *in vitro*. Nevertheless, the important result here is that the model tumors *in vivo* do form a cluster and they are distinct from the normal cluster. This is promising and suggests that breast cancer discrimination on the basis of functional imaging may indeed be possible.

5. SUMMARY

The *in vitro* and *in vivo* experiments performed strongly indicate that probing the oxygenation saturation of hemoglobin of the breast can provide a possible marker for distinguishing cancer from normal tissue and benign processes like fibrocystic disease. Fibroadenoma appears to be a false positive as it is for X-ray mammography and MRI. These results were harnessed in the design of a breast imager based on the modulation of light by ultrasound and may have potential as a diagnostic aid in a minimally invasive environment (22). It is important to note here that functional diagnostics using absorption spectroscopy performs equally well in fatty and fibroglandular breasts. Any imager or diagnostic device incorporating this technique would thus be an asset in the subpopulation of women with radiographically dense breasts.

Certainly, the area is ripe for further development and resolution of the inevitable issues that arise. One such issue is the fact that the depth of penetration of light is poor in the visible region which these studies concentrated on. Signal-to-noise considerations would dictate that a whole breast imager use near infrared light with its better tissue penetration; the 760 nm deoxyhemoglobin absorption resonance is a good candidate for spectral discrimination. For the minimally invasive environment, however, such as at the end of a biopsy needle (22), where signal-to-noise would not be an issue, the stronger resonances at 555 nm, 542 and 576 nm may be used.

6. ACKNOWLEDGEMENTS

The breast biopsy samples were obtained from Dr. H. Singh at Ellis Hospitial in Schenectady, NY. In the initial phases of the project, pathologist Dr. Maleka Hussain supplied breast biopsies, formalin fixed breast tissue and prepared slide mounted samples for optical extinction measurements. Dr. Hussain also provided a second diagnosis of the pathology of selected samples thereby allowing an assessment of errors caused by the heterogeneity of the samples. The mouse model tumors were implanted and grown by M. Huang in the laboratories of D. J. Castro, M.D., Ph. D. and R. Saxton, Ph. D. at UCLA School of Medicine. N. Joongwaard, T. L. Pusheck, M.D and M. Huang of Dr. Castro's group handled the mice during the *in vivo* model tumor experiments which were performed in their laboratories in Los Angeles. Dr. Puscheck performed the surgery on the mice. Many long and informative sessions were held with Dr. Saxton which aided in the understanding and the design of the *in vivo* spectroscopic experiments on the nude mice. The cancer cell cultures were prepared by Drs. C. Keese and I. Giaever at Rensselaer Polytechnic Institute. The Guided Wave remote spectrophotometer was loaned by Mr. David Geller, manufacturer's representative of the Perstorp NIR Group.

7. REFERENCES

1. Fiskin J. B., E. Gratton: Propagation of photon-density waves in strongly scattering media containing an absorbing semi-infinite plane bounded by a straight edge. *J. Opt. Soc. Am. A* 10, 127 - 140, (1993).

2. Sevick E. M., J. Weng, M. Maris, B. Chance: Analysis of absorption, scattering and hemoglobin saturation using phase Modulation spectroscopy. In: Proc. SPIE Time Resolved Spectroscopy and Imaging of Tissues, Eds: B. Chance, A. Katzir. 1431, 264 - 275 (1991).

3. Chance B.: Time resolved spectroscopic (TRS) and continuous wave (CWS) studies of photon migration in human arms and limbs. *Adv. Exp. Med. Biol.* 248, 21 - 31, (1989).

4. Sevick E. M., B. Chance, J. Leigh, S. Nioka, M. Maris: Quantitation of time- and frequency- resolved optical spectra for the determination of tissue oxygenation. *Anal. Biochem*. 195, 330 - 351 (1990).

5. Hebden J. C.: Evaluating the spatial resolution performance of a time-resolved optical imaging system. *Med. Phys.* 19, 1081 - 1087 (1992).

6. de Haller B., C. Depeursinge: Time-Resolved transillumination - Monte-Carlo simulation and comparison with experimental results. In: Proc. SPIE Photon Migration and Imaging in Random Media and Tissues. Eds: B. Chance, R. R. Alfano. 1888, 191 - 200 (1993).

7. Toida M: Measurement of weak light signal buried in scattered light: Realization of Biophoto-CT. *BME* 4, 12 - 23, (1990).

8. Marks F.A., H. W. Tomlinson, G. W. Brooksby: A comprehensive approach to breast cancer detection using

light: photon localization by ultrasound modulation and tissue characterization by spectral discrimination. In: Proc. SPIE Photon Migration and Imaging in Random Media and Tissues. Eds: B. Chance, R. R. Alfano. 1888, 500 - 510, (1993).

9. Wang et. al., Continuous-wave ultrasonic modulation of scattered laser light to image objects in turbid media. *Opt. Lett*. 20, 629 - 631 (1995).

10. Kempe M., A. Z. Genack: Acousto-optic tomography with multiply-scattered light. In press.

11. Leutz W., G. Maret: Ultrasonic modulation of multiply scattered light. *Physica B* 204, 14 - 19, (1995).

12. Yang Y, A. Katz, E. J. Celmer, M. Zurawska-Szczepaniak, R. R. Alfano: Optical spectroscopy of benign and malignant breast tissues. *Lasers in Life Sciences* 7(2), 115 - 127 (1996).

13. Hung J, S Lam, J. C. Riche, B. Palcic: Autofluorescence of normal and malignant bronchial tissue. *Lasers Surg. Med.* 11, 99 - 105 (1991).

14. Yang Y, A. Katz, E. J. Celmer, M. Zurawska-Szczepaniak, R. R. Alfano: Excitation spectrum of malignant and benign breast tissues: A potential optical biopsy approach. *Lasers in Life Sciences* 7(4), 249 - 265 (1997).

15. Richards-Kortum R, R. P. Rava, R. Cothren, A. Metha, M. Fitzmaurice, N. B. Ratliff, J. R. Kramer, C. Kittrell, M. S. Feld: A model for extraction of diagnostic information from laser induced fluorescence spectra of human artery wall. *Spectrochimica Acta* 45A, 87 - 93 (1989).

16. Povlsen C. O.: Heterotransplants of human tumors in nude mice. *Antibiotics Chemother*. 28, 15 - 20 (1980).

17. Vaupel P, H. P. Fortmeyer, S. Rnukel, F. Kallinowski: Blood flow, oxygen consumption and tissue oxygenation of human breast cancer xenografts in nude rats. *Cancer Res*. 47, 3496 - 3503 (1987).

18. Spang-Thomsen M, K. Ryaard, L. Hansen, A. -C. Halvorsen, L. L. Vindelov, N. Brunner: Growth kinetics of four human breast carcinomas grown in nude mice. *Breast Can. Res. Treat*. 14, 235 - 243 (1989).

19. Van Assendelft O.W.: Spectrophotometry of haemoglobin derivatives. Royal Vangorcum Ltd., (1970).

20. Vaupel P.: Oxygenation of Human Tumors. *Strahlenther. Onkol*. 166, 377 - 386 (1990).

21. Rockwell, A., J. E. Moulder: Hypoxic fractions of human tumors xenografted into mice: a review. *Int. J. Radiation Oncology Biol. Phys*. 19, 197 - 202 (1990).

22. Tiemann, J. J, F. A. Marks: US Patent No. 5,349,954: Tumor Tissue Characterization Apparatus and Method (1994).

Send correspondence to: Dr. Fay A. Marks, Bldg. KW, Rm. C608, General Electric Corporate Research and Development, One Research Circle, Niskayuna, NY 12309.

Tel:(518) 387-6757, Fax:(518) 387-5975,E-mail: marks@crd.ge.com

Key words: Optical absorption spectroscopy, Human cancer xenografts, Breast, Tissue biopsy, Hemoglobin.